Sebastian Franz; Fang Liu; Hans-Görg Roos; Martin Stynes; Aihui Zhou

The combination technique for a two-dimensional convection-diffusion problem with exponential layers

Applications of Mathematics, Vol. 54 (2009), No. 3, 203--223

Persistent URL: `http://dml.cz/dmlcz/140360`

THE COMBINATION TECHNIQUE FOR A TWO-DIMENSIONAL CONVECTION-DIFFUSION PROBLEM WITH EXPONENTIAL LAYERS*

Sebastian Franz, Dresden, Fang Liu, Beijing, Hans-Görg Roos, Dresden,
Martin Stynes, Cork, Aihui Zhou, Beijing

Dedicated to Ivan Hlaváček on the occasion of his 75th birthday

Abstract. Convection-diffusion problems posed on the unit square and with solutions displaying exponential layers are solved using a sparse grid Galerkin finite element method with Shishkin meshes. Writing N for the maximum number of mesh intervals in each coordinate direction, our "combination" method simply adds or subtracts solutions that have been computed by the Galerkin FEM on $N \times \sqrt{N}$, $\sqrt{N} \times N$ and $\sqrt{N} \times \sqrt{N}$ meshes. It is shown that the combination FEM yields (up to a factor $\ln N$) the same order of accuracy in the associated energy norm as the Galerkin FEM on an $N \times N$ mesh, but it requires only $\mathcal{O}(N^{3/2})$ degrees of freedom compared with the $\mathcal{O}(N^2)$ used by the Galerkin FEM. An analogous result is also proved for the streamline diffusion finite element method.

Keywords: convection-diffusion, finite element, Shishkin mesh, two-scale discretization

MSC 2010: 65N15, 65N30, 65N55, 65F10, 65Y10

1. Introduction

We consider the singularly perturbed boundary value problem

$$Lu := -\varepsilon\Delta u + \mathbf{b}\cdot\nabla u + cu = f \quad \text{in } \Omega = (0,1)^2, \tag{1.1 a}$$

$$u = 0 \quad \text{on } \partial\Omega, \tag{1.1 b}$$

where ε is a small positive parameter and

$$c(x,y) - \frac{1}{2}\operatorname{div}\mathbf{b}(x,y) \geqslant c_0 > 0 \quad \text{on } \bar{\Omega}, \tag{1.2}$$

* This work was supported by the National Natural Science Foundation of China (10701083 and 10425105), the Chinese National Basic Research Program (2005CB321704) and the Boole Centre for Research in Informatics at National University of Ireland Cork.

where c_0 is a constant. We assume that the functions $\mathbf{b}$, c and f are sufficiently smooth. These hypotheses ensure that (1.1) has a unique solution in $H_0^1(\Omega) \cap H^2(\Omega)$ for all $f \in L^2(\Omega)$.

Write $\mathbf{b}(x,y) = (b_1(x,y), b_2(x,y))$. We shall assume that on $\bar{\Omega}$ one has

$$b_1(x,y) > \beta_1 > 0 \quad \text{and} \quad b_2(x,y) > \beta_2 > 0, \tag{1.3}$$

where β_1 and β_2 are constants. This problem is analysed in Section 2. Its solution contains only exponential and corner layers.

Note that for sufficiently small ε, the hypothesis (1.3) implies that (1.2) can always be ensured by the simple change of variable $v(x,y) = \mathrm{e}^{-\gamma x} u(x,y)$ when γ is chosen suitably independently of ε.

The presence of layers means that special layer-adapted meshes are a good way of computing accurate approximations of the solution of (1.1). Using a priori knowledge of the layer behaviour we shall construct piecewise-uniform meshes—the so-called Shishkin meshes—that resolve most of the layers and yield uniform convergence (i.e., convergence that is independent of the value of the diffusion parameter ε).

On these meshes two finite element discretizations that use bilinear trial and test functions will be analysed: the standard Galerkin FEM and the streamline diffusion FEM (SDFEM), which is also known as the SUPG method.

For problems of type (1.1)–(1.3) where only exponential layers appear, both methods on Shishkin meshes are well understood. For the Galerkin method uniform convergence of almost first order in the energy norm was established by Stynes and O'Riordan [22], while Zhang [27] and Linß [10] proved uniform superconvergence of almost second order in discrete versions of that norm. The SDFEM was studied by Stynes and Tobiska [23] who proved uniform superconvergence in the streamline diffusion norm of almost second order.

In this paper we shall introduce the two-scale finite element discretization scheme, which was first proposed by Liu and Zhou [14], [15] for a class of elliptic boundary value and eigenvalue problems, to solve the 2-dimensional convection-diffusion problem (1.1) using Shishkin meshes. This two-scale finite element method is closely related to the sparse grid method that was developed by Zenger [26], where the multilevel basis of Yserentant [25] was used. Zenger's sparse grid method is a powerful tool in the numerical solution of classical partial differential equations (see [2], [3] and references cited therein). The so-called (multi-scale) combination technique [5], [8], an extrapolation-type sparse grid variant, has been investigated in a number of papers (see, e.g., [2], [7], [8], [20] and numerical experiments for singularly perturbed problems in [18]). Instead of the multi-level basis approach [1], [25], a two-level basis approach in the two-scale finite element discretization was used in [14], [15], [16], which is known to be more flexible than the multi-level basis approach [9], [24].

The main idea of two-scale finite element methods is to use a coarse grid to approximate the low frequencies and to combine some univariate fine and coarse grids to handle the high frequencies by parallel procedures. A method from this class is applied to a singularly perturbed reaction-diffusion problem in [13]; it uses a non-standard basis of piecewise bilinears for the two-scale sparse finite-element space. In the present paper we analyse a related but much simpler combination technique that uses a standard piecewise bilinear finite element space. As far as we know this is the first paper analysing this technique for a singularly perturbed problem.

The paper is organized as follows. In Section 2, some basic notation and terminology are introduced. In Section 3 we describe and analyse the combination finite element approach for convection-diffusion problems with exponential layers; the standard Galerkin and streamline diffusion methods are considered. Finally, in Section 4, numerical results that support our theory are presented.

1.1. Notation

Let $\Omega = (0,1)^2$. We use standard notation (see, e.g., [4]) for the Sobolev spaces $W^{s,p}(\Omega)$ and their associated norms and seminorms. For $p = 2$, set $H^s(\Omega) = W^{s,2}(\Omega)$ and $\|\cdot\|_{s,\Omega} = \|\cdot\|_{s,2,\Omega}$; let $H_0^1(\Omega) = \{v \in H^1(\Omega)\colon\ v|_{\partial\Omega} = 0\}$, where $v|_{\partial\Omega} = 0$ in the sense of traces.

Define an ε-weighted energy norm by

$$|\!|\!|v|\!|\!|_\varepsilon = \{\varepsilon\|\nabla v\|_{0,\Omega}^2 + \|v\|_{0,\Omega}^2\}^{1/2} \quad \forall\, v \in H^1(\Omega).$$

Throughout this paper, the letter C (with or without subscripts) will denote a generic positive constant that may stand for different values at different places.

2. Problem with exponential boundary layers

Throughout Section 2 we assume that (1.3) is valid.

2.1. Solution decomposition

For the analysis we shall assume that the solution u can be decomposed in a way that reflects the typical behaviour that is observed in solutions of (1.1)–(1.3) when interior layers are absent. The precise hypotheses follow.

Assumption 2.1. Suppose that

$$u = S + E_{21} + E_{12} + E_{22}, \tag{2.1}$$

where there exists a constant C such that for all $(x,y)\in\Omega$ and $0\leqslant i+j\leqslant 3$ we have

$$\Bigl|\frac{\partial^{i+j}S}{\partial x^i\partial y^j}(x,y)\Bigr|\leqslant C,\quad \Bigl|\frac{\partial^{i+j}E_{22}}{\partial x^i\partial y^j}(x,y)\Bigr|\leqslant C\varepsilon^{-(i+j)}\mathrm{e}^{-(\beta_1(1-x)+\beta_2(1-y))/\varepsilon},$$
$$\Bigl|\frac{\partial^{i+j}E_{21}}{\partial x^i\partial y^j}(x,y)\Bigr|\leqslant C\varepsilon^{-i}\mathrm{e}^{-\beta_1(1-x)/\varepsilon},\quad \Bigl|\frac{\partial^{i+j}E_{12}}{\partial x^i\partial y^j}(x,y)\Bigr|\leqslant C\varepsilon^{-j}\mathrm{e}^{-\beta_2(1-y)/\varepsilon}$$

and for $i+j=4$ we have the L_2 bounds

$$\Bigl\|\frac{\partial^{i+j}S}{\partial x^i\partial y^j}(x,y)\Bigr\|_{0,\Omega}\leqslant C,\qquad \Bigl\|\frac{\partial^{i+j}E_{21}}{\partial x^i\partial y^j}(x,y)\Bigr\|_{0,\Omega}\leqslant C\varepsilon^{-i+1/2},\tag{2.2 a}$$
$$\Bigl\|\frac{\partial^{i+j}E_{12}}{\partial x^i\partial y^j}(x,y)\Bigr\|_{0,\Omega}\leqslant C\varepsilon^{-j+1/2},\quad \Bigl\|\frac{\partial^{i+j}E_{22}}{\partial x^i\partial y^j}(x,y)\Bigr\|_{0,\Omega}\leqslant C\varepsilon^{1-i-j}.\tag{2.2 b}$$

Here S is the smooth part of u, E_{21} is an exponential boundary layer along the side $x=1$ of Ω, E_{12} is an exponential boundary layer along the side $y=1$, while E_{22} is an exponential corner layer at (1,1). In [12, Theorem 5.1] sufficient conditions are given (in the case of a constant-coefficient differential operator) for these conditions to hold; see also [19].

2.2. The Shishkin mesh

In this subsection we describe the Shishkin mesh. Shishkin meshes are piecewise-uniform meshes, constructed a priori, that are refined inside layers. See [11], [17], [21] for a detailed discussion of their properties and uses.

Let N be an even positive integer. We let λ_x and λ_y denote two mesh transition parameters that will be used to specify where the mesh changes from coarse to fine: they are defined by

$$\lambda_x=\min\Bigl\{\frac12,\ \sigma\frac{\varepsilon}{\beta_1}\ln N\Bigr\}\quad\text{and}\quad \lambda_y=\min\Bigl\{\frac12,\ \sigma\frac{\varepsilon}{\beta_2}\ln N\Bigr\}.\tag{2.3}$$

In (2.3) different authors make various choices for the multiplier σ; the value chosen is often equal to the order of convergence of the method. In our analysis we postpone the choice of σ for as long as possible in order to see its effect on the two-scale analysis.

Assumption 2.2. Suppose that $\varepsilon\leqslant CN^{-1}$, as otherwise the analysis can be carried out using standard classical techniques.

Then without loss of generality one can assume that N is so large that

$$\lambda_x=(\sigma\varepsilon\ln N)/\beta_1\quad\text{and}\quad \lambda_y=(\sigma\varepsilon\ln N)/\beta_2.\tag{2.4}$$

Partition of Ω as in Fig. 1: $\bar{\Omega} = \Omega_{11} \cup \Omega_{21} \cup \Omega_{12} \cup \Omega_{22}$, where

$$\Omega_{11} = [0, 1-\lambda_x] \times [0, 1-\lambda_y], \quad \Omega_{21} = [1-\lambda_x, 1] \times [0, 1-\lambda_y],$$
$$\Omega_{12} = [0, 1-\lambda_x] \times [1-\lambda_y, 1], \quad \Omega_{22} = [1-\lambda_x, 1] \times [1-\lambda_y, 1].$$

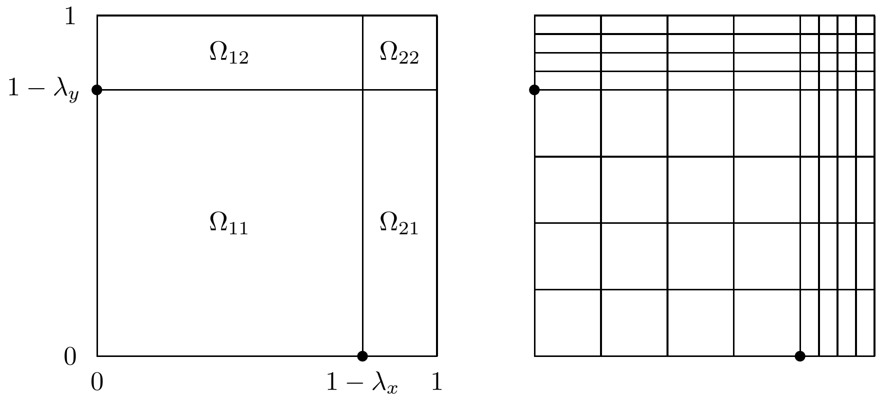

Figure 1. Shishkin mesh for convection-diffusion with two outflow exponential layers.

The mesh points $\Omega^N = \{(x_i, y_j) \in \bar{\Omega} \colon\ i, j = 0, \dots, N\}$ form the rectangular lattice defined by

(2.5 a)
$$x_i = \begin{cases} 2i(1-\lambda_x)/N & \text{for } i = 0, \dots, N/2, \\ 1 - 2(N-i)\lambda_x/N & \text{for } i = N/2+1, \dots, N, \end{cases}$$

and

(2.5 b)
$$y_j = \begin{cases} 2j(1-\lambda_y)/N & \text{for } j = 0, \dots, N/2, \\ 1 - 2(N-j)\lambda_y/N & \text{for } j = N/2+1, \dots, N. \end{cases}$$

The mesh sizes $h_i := x_i - x_{i-1}$ and $k_j := y_j - y_{j-1}$ satisfy

(2.6 a)
$$h_i = \begin{cases} \hbar_1 := \dfrac{2(1-\lambda_x)}{N} & \text{for } i = 0, \dots, N/2, \\ \hbar_2 := \dfrac{2\sigma\varepsilon \ln N}{\beta_1 N} & \text{for } i = N/2+1, \dots, N, \end{cases}$$

and

(2.6 b)
$$k_j = \begin{cases} \kappa_1 := \dfrac{2(1-\lambda_y)}{N} & \text{for } j = 0, \dots, N/2, \\ \kappa_2 := \dfrac{2\sigma\varepsilon \ln N}{\beta_2 N} & \text{for } j = N/2+1, \dots, N. \end{cases}$$

Our mesh is constructed by drawing lines parallel to the coordinate axes through these mesh points, so it is a tensor product of two one-dimensional piecewise uniform meshes. This divides Ω into a set $T^{N,N}$ of mesh rectangles K whose sides are parallel to the axes—see Fig. 1. The mesh is coarse on Ω_{11}, coarse/fine on $\Omega_{21} \cup \Omega_{12}$, and fine on Ω_{22}. The mesh is quasi-uniform on Ω_{11} and its diameter d satisfies there $\sqrt{2}/N \leqslant d \leqslant 2\sqrt{2}/N$; on $\Omega_{12} \cup \Omega_{21}$, each mesh rectangle has dimensions $\mathcal{O}(N^{-1})$ by $\mathcal{O}(\varepsilon N^{-1} \ln N)$; and on Ω_{22} each rectangle is $\mathcal{O}(\varepsilon N^{-1} \ln N)$ by $\mathcal{O}(\varepsilon N^{-1} \ln N)$. We shall use these properties several times in our analysis. Given a mesh rectangle K, its dimensions are written as $h_{x,K}$ by $h_{y,K}$ and its barycentre is denoted by (x_K, y_K).

2.3. Interpolation

Problem (1.1) will be discretized using a two-scale finite element method. Its analysis requires information regarding the two-scale interpolation error which will be derived in this subsection.

Let N_x be an even positive integer that satisfies $N_x \leqslant N$. Let λ_x be specified by (2.4), which depends on N but not on N_x. Write $T^{N_x}[0,1]$ for the piecewise-uniform mesh on $[0,1]$ specified by (2.5 a) with $N = N_x$. Let $V^{N_x}[0,1] \subset H^1(0,1)$ be the associated piecewise linear finite element space. Set $V_0^{N_x}[0,1] = V^{N_x}[0,1] \cap H_0^1(0,1)$. Let $I_N\colon C[0,1] \to V^{N_x}[0,1]$ be the standard piecewise linear Lagrange interpolation operator associated with $T^N[0,1]$.

We invoke the standard interpolation analysis. Let $p \in [2,\infty]$ and $v \in W^{2,p}(0,1)$. Then the piecewise linear interpolant $I_N v$ of v satisfies the bounds

$$\begin{aligned} (2.7) \qquad & \|v - I_N v\|_{L^p(x_{i-1},x_i)} + h_i \|(v - I_N v)'\|_{L^p(x_{i-1},x_i)} \\ & \qquad \leqslant C \min\bigl\{h_i \|v'\|_{L^p(x_{i-1},x_i)},\, h_i^2 \|v''\|_{L^p(x_{i-1},x_i)}\bigr\}, \end{aligned}$$

where $h_i := x_i - x_{i-1}$ for $i = 1, \ldots, N$. Although the problem (1.1) is posed in two dimensions, our interpolation analysis requires only the one-dimensional interpolation inequality (2.7).

Let N_y be an even positive integer satisfying $N_Y \leqslant N$; now the y-axis interval $[0,1]$ is subdivided into N_y intervals using (2.5 b) with $N = N_y$, and λ_y specified by (2.4). Define the rectangular mesh $T^{N_x,N_y}(\Omega) = T^{N_x}[0,1] \times T^{N_y}[0,1]$. Set $V^{N_x,N_y}(\Omega) = V^{N_x}[0,1] \times V^{N_y}[0,1]$ and $V_0^{N_x,N_y}(\Omega) = V_0^{N_x}[0,1] \times V_0^{N_y}[0,1]$. The following inverse inequality, which follows easily from standard inverse inequalities in one dimension, will be used in our analysis:

$$h_x \Bigl\|\frac{\partial v}{\partial x}\Bigr\|_{0,K} + k_y \Bigl\|\frac{\partial v}{\partial y}\Bigr\|_{0,K} \leqslant \|v\|_{0,K} \quad \forall\, v \in V^{N_x,N_y}(\Omega),\ \forall\, K \in T^{N_x,N_y}(\Omega),$$

where the rectangle K has dimensions $h_x \times k_y$.

Let $I_{N_x,N_y}\colon C(\bar{\Omega}) \to V^{N_x,N_y}(\Omega)$ be the usual piecewise-bilinear interpolation operator on $T^{N_x,N_y}(\Omega)$. Write $I_{N_x,0}$ for the interpolation operator that interpolates only in the x-direction at the mesh points (2.5 a), so $I_{N_x,0}\colon C(\bar{\Omega}) \to V^{N_x}[0,1] \times C[0,1]$. Similarly, let $I_{0,N_y}\colon C(\bar{\Omega}) \to C[0,1] \times V^{N_y}[0,1]$ interpolate only in the y-direction at the mesh points (2.5 b). Then clearly

$$I_{N_x,N_y} = I_{N_x,0} \circ I_{0,N_y} = I_{0,N_y} \circ I_{N_x,0}, \tag{2.8 a}$$

$$\frac{\partial}{\partial x} I_{N_x,N_y} = I_{0,N_y} \circ \frac{\partial}{\partial x} I_{N_x,0}, \tag{2.8 b}$$

$$\frac{\partial}{\partial y} I_{N_x,N_y} = I_{N_x,0} \circ \frac{\partial}{\partial y} I_{0,N_y}. \tag{2.8 c}$$

Let $\hat{N} < N$ be a positive even integer that for the present is unspecified. When we use a Shishkin mesh on Ω with $\hat{N}$ intervals instead of N in one or both coordinate directions, we shall retain the same values of λ_x and λ_y as in (2.4), so the regions Ω_{ij} remain the same but the number of elements in the subdivision of these regions has changed. The mesh sizes in the x and y directions are now denoted by $\hat{h}_i$ and $\hat{k}_j$ respectively; their values are given by replacing N by $\hat{N}$ in (2.6 a) and (2.6 b), except that the $\ln N$ factor remains unchanged.

Finally, define $V^N_{\hat{N},\hat{N}} = \operatorname{span}\{V^{N,\hat{N}}(\Omega), V^{\hat{N},N}(\Omega), V^{\hat{N},\hat{N}}(\Omega)\}$ and the two-scale interpolation operator $I^N_{\hat{N},\hat{N}}\colon C(\bar{\Omega}) \to V^N_{\hat{N},\hat{N}}$ by

$$I^N_{\hat{N},\hat{N}} u = I_{N,\hat{N}} u + I_{\hat{N},N} u - I_{\hat{N},\hat{N}} u. \tag{2.9}$$

In the remainder of this section we show that the standard one-scale interpolation, which uses $I_{N,N}$ on the full Shishkin mesh, can be approximated accurately by the two-scale interpolation (2.9) for a suitable choice of $\hat{N}$ that satisfies $\hat{N} \ll N$, and consequently (2.9) is more economical than $I_{N,N}$.

Lemma 2.3. *There exists a constant C such that*

$$\|I^N_{\hat{N},\hat{N}} u - I_{N,N} u\|_0 \leqslant C[N^{-\sigma} + \hat{N}^{-4}].$$

Proof. Recall that $u = S + E_{21} + E_{12} + E_{22}$ by Assumption 2.1. Using the identity

$$I_{N,N} - I^N_{\hat{N},\hat{N}} = (I_{N,0} - I_{\hat{N},0})(I_{0,N} - I_{0,\hat{N}}),$$

we have

$$I_{N,N} u - I^N_{\hat{N},\hat{N}} u = (I_{N,0} - I_{\hat{N},0})(I_{0,N} - I_{0,\hat{N}})(S + E_{21} + E_{12} + E_{22}).$$

We analyse separately the four terms on the right-hand side. For the first term one has

$$\|(I_{N,0}-I_{\hat N,0})(I_{0,N}-I_{0,\hat N})S\|_{0,\Omega} \leqslant C\hat N^{-2}\Big\|(I_{0,N}-I_{0,\hat N})\frac{\partial^2 S}{\partial x^2}\Big\|_{0,\Omega} \leqslant C\hat N^{-4}\Big\|\frac{\partial^4 S}{\partial x^2\partial y^2}\Big\|_{0,\Omega} \leqslant C\hat N^{-4}.$$

For the second term,

$$\|(I_{N,0}-I_{\hat N,0})(I_{0,N}-I_{0,\hat N})E_{21}\|_{0,\Omega_{11}\cup\Omega_{12}} \leqslant C\|E_{21}\|_{\infty,\Omega_{11}\cup\Omega_{12}} \leqslant C\max_{(x,y)\in\Omega_{11}\cup\Omega_{12}} \mathrm{e}^{-\beta_1(1-x)/\varepsilon}.$$

Since $x\in[0,1-\lambda_x]$, by (2.4) we get

$$\|(I_{N,0}-I_{\hat N,0})(I_{0,N}-I_{0,\hat N})E_{21}\|_{0,\Omega_{11}\cup\Omega_{12}} \leqslant CN^{-\sigma}. \tag{2.10}$$

Next, consider the error on $\Omega_{21}\cup\Omega_{22}=[1-\lambda_x,1]\times[0,1]$. Using (2.8 a) and Assumption 2.1, we obtain

$$\begin{aligned}\|(I_{N,0}-I_{\hat N,0})&(I_{0,N}-I_{0,\hat N})E_{21}\|_{0,\Omega_{21}\cup\Omega_{22}}\\ &\leqslant C\hat\hbar_2^2\Big\|(I_{0,N}-I_{0,\hat N})\frac{\partial^2 E_{21}}{\partial x^2}\Big\|_{0,\Omega_{21}\cup\Omega_{22}}\\ &\leqslant C\hat\hbar_2^2\hat N^{-2}\Big\|\frac{\partial^4 E_{21}}{\partial x^2\partial y^2}\Big\|_{0,\Omega_{21}\cup\Omega_{22}} \leqslant C\hat\hbar_2^2\hat N^{-2}\varepsilon^{-3/2}.\end{aligned}$$

However, $\hat\hbar_2\leqslant C\varepsilon\hat N^{-1}\ln N$ by (2.4), so this yields

$$\|(I_{N,0}-I_{\hat N,0})(I_{0,N}-I_{0,\hat N})E_{21}\|_{0,\Omega_{21}\cup\Omega_{22}} \leqslant C\varepsilon^{1/2}\hat N^{-4}(\ln N)^2.$$

One obtains similarly

$$\|(I_{N,0}-I_{\hat N,0})(I_{0,N}-I_{0,\hat N})E_{12}\|_{0,\Omega_{11}\cup\Omega_{21}} \leqslant CN^{-\sigma}$$

and

$$\|(I_{N,0}-I_{\hat N,0})(I_{0,N}-I_{0,\hat N})E_{12}\|_{0,\Omega_{12}\cup\Omega_{22}} \leqslant C\varepsilon^{1/2}\hat N^{-4}(\ln N)^2.$$

For the last term, we have

$$\|(I_{N,0}-I_{\hat N,0})(I_{0,N}-I_{0,\hat N})E_{22}\|_{0,\Omega\setminus\Omega_{22}} \leqslant C\|E_{22}\|_{\infty,\Omega\setminus\Omega_{22}} \leqslant C\max_{(x,y)\in\Omega\setminus\Omega_{22}} \mathrm{e}^{-(\beta_1(1-x)+\beta_2(1-y))/\varepsilon}.$$

Then from (2.4) it follows that

$$\|(I_{N,0} - I_{\hat{N},0})(I_{0,N} - I_{0,\hat{N}})E_{22}\|_{0,\Omega\setminus\Omega_{22}} \leqslant CN^{-\sigma}. \tag{2.11}$$

On $\Omega_{22} = [1-\lambda_x, 1] \times [1-\lambda_y, 1]$, Assumption 2.1 yields

$$\begin{aligned}\|(I_{N,0} - I_{\hat{N},0})(I_{0,N} - I_{0,\hat{N}})E_{22}\|_{0,\Omega_{22}} &\leqslant C\hat{\hbar}_2^2\hat{\kappa}_2^2\Big\|\frac{\partial^4 E_{22}}{\partial x^2\partial y^2}\Big\|_{0,\Omega_{22}}\\ &\leqslant C\hat{\hbar}_2^2\hat{\kappa}_2^2\varepsilon^{-3} \leqslant C\varepsilon\hat{N}^{-4}(\ln N)^4,\end{aligned}$$

since $\hat{\hbar}_2 \leqslant C\varepsilon\hat{N}^{-1}\ln N$ and $\hat{\kappa}_2 \leqslant C\varepsilon\hat{N}^{-1}\ln N$ by (2.4).

Combining these bounds gives

$$\|I^N_{\hat{N},\hat{N}}u - I_{N,N}u\|_0 \leqslant C(N^{-\sigma} + \hat{N}^{-4}(1 + \varepsilon^{1/2}(\ln N)^2 + \varepsilon(\ln N)^4)).$$

Recalling that $\varepsilon \leqslant N^{-1}$, the result follows. □

Remark 2.4. In the analysis of Lemma 2.3 bounds on the 4th-order derivatives are used. Alternatively, the L_2-interpolation error could be bounded using only the 3rd-order derivatives. One then obtains

$$\|I^N_{\hat{N},\hat{N}}u - I_{N,N}u\|_0 \leqslant C[N^{-\sigma} + \hat{N}^{-3}].$$

Next we consider the error in the weighted H^1 seminorm.

Lemma 2.5. *There exists a constant C such that*

$$\varepsilon^{1/2}\|\nabla(I^N_{\hat{N},\hat{N}}u - I_{N,N}u)\|_0 \leqslant C[\varepsilon^{1/2}N^{1-\sigma} + N^{-\sigma}(\ln N)^{1/2} + \hat{N}^{-3}\ln N].$$

Proof. As $u = S + E_{21} + E_{12} + E_{22}$, we have

$$\begin{aligned}&\varepsilon^{1/2}\|\nabla(I^N_{\hat{N},\hat{N}}u - I_{N,N}u)\|_{0,\Omega}\\ &\qquad = \varepsilon^{1/2}\|\nabla((I_{N,0} - I_{\hat{N},0})(I_{0,N} - I_{0,\hat{N}})(S + E_{21} + E_{12} + E_{22}))\|_{0,\Omega}.\end{aligned}$$

We shall analyse separately each of the four terms on the right-hand side, using Assumption 2.1 in each case. For the first term, by (2.8) and (2.2) one has

$$\begin{aligned}\varepsilon^{1/2}\Big\|\frac{\partial}{\partial x}(I_{N,0} - I_{\hat{N},0})(I_{0,N} - I_{0,\hat{N}})S\Big\|_{0,\Omega} &\leqslant C\varepsilon^{1/2}\hat{N}^{-1}\Big\|(I_{0,N} - I_{0,\hat{N}})\frac{\partial^2 S}{\partial x^2}\Big\|_{0,\Omega}\\ &\leqslant C\varepsilon^{1/2}\hat{N}^{-3}\Big\|\frac{\partial^4 S}{\partial x^2\partial y^2}\Big\|_{0,\Omega} \leqslant C\varepsilon^{1/2}\hat{N}^{-3}.\end{aligned}$$

For the second term, an inverse estimate, (2.8) and (2.10) yield

$$\varepsilon^{1/2}\Big\|\frac{\partial}{\partial x}(I_{N,0}-I_{\hat N,0})(I_{0,N}-I_{0,\hat N})E_{21}\Big\|_{0,\Omega_{11}\cup\Omega_{12}} \leqslant C\varepsilon^{1/2}N\|(I_{N,0}-I_{\hat N,0})(I_{0,N}-I_{0,\hat N})E_{21}\|_{0,\Omega_{11}\cup\Omega_{12}} \leqslant C\varepsilon^{1/2}N^{1-\sigma}.$$

The function E_{21} is bounded on $\Omega_{21}\cup\Omega_{22}=[1-\lambda_x,1]\times[0,1]$ by using (2.8), (2.7) and (2.2):

$$\begin{aligned}\varepsilon^{1/2}\Big\|\frac{\partial}{\partial x}(I_{N,0}-I_{\hat N,0})(I_{0,N}-I_{0,\hat N})E_{21}\Big\|_{0,\Omega_{21}\cup\Omega_{22}} &\leqslant C\varepsilon^{1/2}(\varepsilon\hat N^{-1}\ln N)\Big\|(I_{0,N}-I_{0,\hat N})\frac{\partial^2E_{21}}{\partial x^2}\Big\|_{0,\Omega_{21}\cup\Omega_{22}}\\ &\leqslant C\varepsilon^{3/2}\hat N^{-3}(\ln N)\Big\|\frac{\partial^4E_{21}}{\partial x^2\partial y^2}\Big\|_{0,\Omega_{21}\cup\Omega_{22}} \leqslant C\hat N^{-3}\ln N.\end{aligned}$$

Next, consider the third term. The properties (2.8) and the interpolation error estimate (2.7) yield

$$\begin{aligned}&\varepsilon^{1/2}\Big\|\frac{\partial}{\partial x}(I_{N,0}-I_{\hat N,0})(I_{0,N}-I_{0,\hat N})E_{12}\Big\|_{0,\Omega_{11}\cup\Omega_{21}}\\ &\quad\leqslant C\varepsilon^{1/2}\Big\|(I_{0,N}-I_{0,\hat N})\frac{\partial E_{12}}{\partial x}\Big\|_{0,\Omega_{11}\cup\Omega_{21}}\\ &\quad\leqslant C\varepsilon^{1/2}\Big\|(I_{0,N}-I_{0,\hat N})\frac{\partial E_{12}}{\partial x}\Big\|_{\infty,\Omega_{11}\cup\Omega_{21}}\\ &\quad\leqslant C\varepsilon^{1/2}\Big\|\frac{\partial E_{12}}{\partial x}\Big\|_{\infty,\Omega_{11}\cup\Omega_{21}} \leqslant C\varepsilon^{1/2}\max_{(x,y)\in\Omega_{11}\cup\Omega_{21}}\mathrm{e}^{-\beta_2(1-y)/\varepsilon} \leqslant C\varepsilon^{1/2}N^{-\sigma}.\end{aligned}$$

On $\Omega_{12}\cup\Omega_{22}=[0,1]\times[1-\lambda_y,1]$, we again invoke (2.8), (2.7) and (2.2) to get

$$\begin{aligned}\varepsilon^{1/2}\Big\|\frac{\partial}{\partial x}(I_{N,0}-I_{\hat N,0})(I_{0,N}-I_{0,\hat N})E_{12}\Big\|_{0,\Omega_{12}\cup\Omega_{22}} &\leqslant C\varepsilon^{1/2}\hat N^{-1}\Big\|(I_{0,N}-I_{0,\hat N})\frac{\partial^2E_{12}}{\partial x^2}\Big\|_{0,\Omega_{12}\cup\Omega_{22}}\\ &\leqslant C\varepsilon^{1/2}\hat N^{-1}\hat\kappa_2^2\Big\|\frac{\partial^4E_{12}}{\partial x^2\partial y^2}\Big\|_{0,\Omega_{12}\cup\Omega_{22}} \leqslant C\varepsilon\hat N^{-3}(\ln N)^2.\end{aligned}$$

Finally, for the last term, the properties (2.8), an inverse estimate and (2.11) yield

$$\varepsilon^{1/2}\Big\|\frac{\partial}{\partial x}(I_{N,0}-I_{\hat N,0})(I_{0,N}-I_{0,\hat N})E_{22}\Big\|_{0,\Omega_{11}\cup\Omega_{12}} \leqslant C\varepsilon^{1/2}N^{1-\sigma}.$$

The error in E_{22} on $\Omega_{21} = [1-\lambda_x, 1] \times [0, 1-\lambda_y]$ is bounded as follows:

$$\begin{aligned}
\varepsilon^{1/2}\Big\|\frac{\partial}{\partial x}&(I_{N,0} - I_{\hat N,0})(I_{0,N} - I_{0,\hat N})E_{22}\Big\|_{0,\Omega_{21}} \\
&\leqslant C\varepsilon^{1/2}\Big\|(I_{0,N} - I_{0,\hat N})\frac{\partial E_{22}}{\partial x}\Big\|_{0,\Omega_{21}} \\
&\leqslant C\varepsilon^{1/2}[\operatorname{meas}\Omega_{21}]^{1/2}\Big\|\frac{\partial E_{22}}{\partial x}\Big\|_{\infty,\Omega_{21}} \\
&\leqslant CN^{-\sigma}(\ln N)^{1/2},
\end{aligned}$$

by using the value of λ_y in (2.4). As for the error on $\Omega_{22} = [1-\lambda_x, 1] \times [1-\lambda_y, 1]$, we have

$$\begin{aligned}
\Big\|\frac{\partial}{\partial x}(I_{N,0} - I_{\hat N,0})(I_{0,N} - I_{0,\hat N})E_{22}\Big\|_{0,\Omega_{22}} &\leqslant C\hbar_2\Big\|(I_{0,N} - I_{0,\hat N})\frac{\partial^2 E_{22}}{\partial x^2}\Big\|_{0,\Omega_{22}} \\
&\leqslant C\hbar_2\hat\kappa_2^2\Big\|\frac{\partial^4 E_{22}}{\partial x^2 \partial y^2}\Big\|_{0,\Omega_{22}}.
\end{aligned}$$

Hence, by (2.2) one gets

$$\varepsilon^{1/2}\Big\|\frac{\partial}{\partial x}(I_{N,0} - I_{\hat N,0})(I_{0,N} - I_{0,\hat N})E_{22}\Big\|_{0,\Omega_{22}} \leqslant C\varepsilon^{1/2}\hbar_2\hat\kappa_2^2\varepsilon^{-3} \leqslant C\varepsilon^{1/2}\hat N^{-3}(\ln N)^3.$$

Assembling these bounds and discarding those terms that are dominated by evidently larger terms, we have now shown that

$$\begin{aligned}
\varepsilon^{1/2}\Big\|&\frac{\partial}{\partial x}(I^N_{\hat N,\hat N}u - I_{N,N}u)\Big\|_0 \\
&\leqslant C[\varepsilon^{1/2}N^{1-\sigma} + \hat N^{-3}\ln N + N^{-\sigma}(\ln N)^{1/2} + \varepsilon^{1/2}\hat N^{-3}(\ln N)^3].
\end{aligned}$$

The desired bound on $\varepsilon^{1/2}\|\frac{\partial}{\partial x}(I^N_{\hat N,\hat N}u - I_{N,N}u)\|_0$ now follows using $\varepsilon \leqslant N^{-1}$. The estimates for $\frac{\partial}{\partial y}(I^N_{\hat N,\hat N}u - I_{N,N}u)$ are proved in a similar manner. This completes the proof. □

The main result of this section is now immediate.

Theorem 2.6. *There exists a constant C such that*

$$|||I^N_{\hat N,\hat N}u - I_{N,N}u|||_\varepsilon \leqslant C[\varepsilon^{1/2}N^{1-\sigma} + N^{-\sigma}(\ln N)^{1/2} + \hat N^{-3}\ln N].$$

Proof. By definition

$$|||I^N_{\hat N,\hat N}u - I_{N,N}u|||^2_\varepsilon = \varepsilon\|\nabla(I^N_{\hat N,\hat N}u - I_{N,N}u)\|^2_0 + \|I^N_{\hat N,\hat N}u - I_{N,N}u\|^2_0$$

and Lemmas 2.3 and 2.5 yield the desired result. □

Corollary 2.7. *If $\sigma \geqslant 3/2$ and $\hat{N} \geqslant C_1 N^{1/3}$ for some constant C_1, then there exists a constant C such that*

$$\left|\!\left|\!\left| I^N_{\hat{N},\hat{N}} u - I_{N,N} u \right|\!\right|\!\right|_\varepsilon \leqslant C N^{-1} \ln N. \tag{2.12}$$

The bound on $I^N_{\hat{N},\hat{N}} u - I_{N,N} u$ given in Corollary 2.7 shows that the two-scale interpolant $I^N_{\hat{N},\hat{N}} u$ is computationally a more economical approximation to u than $I_{N,N} u$. Indeed, it is well known [6], [21], [22] that for $\sigma \geqslant 2$ one has

$$|\!|\!| u - I_{N,N} u |\!|\!|_\varepsilon \leqslant C N^{-1} \ln N, \tag{2.13}$$

and this estimate is in general sharp; thus the approximation accuracy of the two-scale interpolant $I^N_{\hat{N},\hat{N}} u$ exhibited in (2.12) is the same as that of the standard interpolant $I_{N,N} u$ up to a factor $\ln N$, even though when $\hat{N} = C_1 N^{1/3}$ the number of degrees of freedom used in $I^N_{\hat{N},\hat{N}} u$ is $\mathcal{O}(N^{4/3})$ while $I_{N,N} u$ requires $\mathcal{O}(N^2)$ degrees of freedom.

3. The combination technique

Throughout this section, the even positive integers N_x and N_y may take the values N or $\hat{N}$, where $\hat{N} = C_1 N^{1/3}$ or $\hat{N} = C_2 N^{1/2}$ for some constants C_1 and C_2. In all cases the same transition points defined by (2.4) are used. The trial space V^{N_x,N_y} is the standard space of continuous piecewise bilinear functions that satisfy the boundary conditions of the problem:

$$V^{N_x,N_y} = \{v \in C(\bar{\Omega}) \colon\ v|_{\partial\Omega} = 0 \text{ and } v|_K \in Q_1(K)\ \forall\, K \in T^{N_x,N_y}\}.$$

The variational formulation of (1.1) is: find $u \in H^1_0(\Omega)$ such that

$$a_{\mathrm{GAL}}(u,v) := \varepsilon(\nabla u, \nabla v) + (b \cdot \nabla u, v) + (cu, v) = (f, v) \quad \forall\, v \in H^1_0(\Omega).$$

This bilinear form is coercive, i.e.,

$$a_{\mathrm{GAL}}(v,v) \geqslant \min\{c_0, 1\} |\!|\!| v |\!|\!|^2_\varepsilon \quad \forall\, v \in H^1_0(\Omega). \tag{3.1}$$

Define the Galerkin finite element approximation $u_{N_x,N_y} \in V^{N_x,N_y}$ of the solution of (1.1) by

$$a_{\mathrm{GAL}}(u_{N_x,N_y}, v_{N_x,N_y}) = (f, v_{N_x,N_y}) \quad \forall\, v_{N_x,N_y} \in V^{N_x,N_y}. \tag{3.2}$$

From (3.1) it follows that (3.2) has a unique solution $u_{N_x,N_y} \in V^{N_x,N_y}$.

Lemma 3.1 [27, proof of Theorem 5.3]. *Choose $\sigma = 5/2$ in (2.4). Then the Galerkin FEM solution $u_{N,N}$ satisfies*

$$\| I_{N,N}u - u_{N,N} \|_\varepsilon \leqslant CN^{-2}\ln^2 N$$

for some constant C.

This result and (2.13) imply that for $\sigma = 5/2$ the Galerkin FEM solution $u_{N,N}$ satisfies

$$\| u - u_{N,N} \|_\varepsilon \leqslant CN^{-1}\ln N. \tag{3.3}$$

Furthermore, it is clear from the arguments of [27] that Lemma 3.1 can be generalized to

$$\| I_{N_x,N_y}u - u_{N_x,N_y} \|_\varepsilon \leqslant CM^{-2}\ln^2 N, \quad \text{where } M = \min\{N_x, N_y\}. \tag{3.4}$$

In the combination technique we compute a two-scale finite element approximation $u^N_{\hat{N},\hat{N}}$ defined by

$$u^N_{\hat{N},\hat{N}} = u_{N,\hat{N}} + u_{\hat{N},N} - u_{\hat{N},\hat{N}}.$$

Note that here for $\hat{N} = N^{1/p}$ each term on the right-hand side is computed from a discrete system that has at most $\mathcal{O}(N^{1+1/p})$ degrees of freedom instead of $\mathcal{O}(N^2)$ used by the standard FEM.

Theorem 3.2. *Choose $\sigma = 5/2$ in (2.4). There exists a constant C such that for $\hat{N} = C_2\sqrt{N}$ one has*

$$\left\| u^N_{\hat{N},\hat{N}} - u_{N,N} \right\|_\varepsilon \leqslant CN^{-1}\ln^2 N \tag{3.5}$$

and

$$\left\| u - u^N_{\hat{N},\hat{N}} \right\|_\varepsilon \leqslant CN^{-1}\ln^2 N. \tag{3.6}$$

P r o o f. The definition of $u^N_{\hat{N},\hat{N}}$ implies that

$$\begin{aligned} u^N_{\hat{N},\hat{N}} - u_{N,N} = {}& u_{N,\hat{N}} - I_{N,\hat{N}}u + u_{\hat{N},N} - I_{\hat{N},N}u - u_{\hat{N},\hat{N}} + I_{\hat{N},\hat{N}}u \\ & - u_{N,N} + I_{N,N}u + I_{N,\hat{N}}u + I_{\hat{N},N}u - I_{\hat{N},\hat{N}}u - I_{N,N}u. \end{aligned}$$

Hence

$$\begin{aligned} \left\| u^N_{\hat{N},\hat{N}} - u_{N,N} \right\|_\varepsilon \leqslant {}& \| u_{N,\hat{N}} - I_{N,\hat{N}}u \|_\varepsilon + \| u_{\hat{N},N} - I_{\hat{N},N}u \|_\varepsilon \\ & + \| u_{\hat{N},\hat{N}} - I_{\hat{N},\hat{N}}u \|_\varepsilon + \| u_{N,N} - I_{N,N}u \|_\varepsilon \\ & + \| I_{N,\hat{N}}u + I_{\hat{N},N}u - I_{\hat{N},\hat{N}}u - I_{N,N}u \|_\varepsilon; \end{aligned}$$

now invoke (3.4) and Corollary 2.7 to complete the proof of (3.5). The bound (3.6) then follows from (3.3) and the triangle inequality. □

R e m a r k 3.3.

(i) From the numerical results in Section 4, it seems that the more economical choice $\hat{N} = C_1 N^{1/3}$ is as accurate as $\hat{N} = C_2 N^{1/2}$, but the proof of this is still open.

(ii) The numerical results indicate supercloseness results for the differences

$$u^N_{\hat{N},\hat{N}} - I^N_{\hat{N},\hat{N}} u \quad \text{and} \quad u^N_{\hat{N},\hat{N}} - I_{N,N} u$$

in the energy norm. If one could prove these results, then the splitting

$$u^N_{\hat{N},\hat{N}} - u = \left(u^N_{\hat{N},\hat{N}} - I^N_{\hat{N},\hat{N}} u\right) + \left(I^N_{\hat{N},\hat{N}} u - u\right)$$

would yield (3.6) directly without invoking (3.4) as in the proof of Theorem 3.2.

R e m a r k 3.4 (Stabilized finite element method). If the standard Galerkin FEM is replaced by a stabilized FEM, the combination technique can also be applied. One can analyse such an approach if a supercloseness result for the stabilized FEM is available. We shall give some results for the streamline diffusion FEM (SDFEM). Therefore, define the bilinear form $a_{\rm SD}(\cdot,\cdot)$ by

$$a_{\rm SD}(w,v) = a_{\rm GAL}(w,v) + \sum_{K\subset\Omega_{11}} \delta_K(-\varepsilon\Delta w + b\cdot\nabla w + cw, b\cdot\nabla v)_K,$$

where $\delta_K \geqslant 0$ is a user-chosen piecewise constant parameter.

Then the SDFEM is defined as follows: find $w_{N_x,N_y} \in V^{N_x,N_y}$ such that

$$a_{\rm SD}(w_{N_x,N_y}, v_{N_x,N_y}) = (f, v_{N_x,N_y}) + \sum_{K\subset\Omega_{11}} \delta_K(f, b\cdot\nabla v_{N_x,N_y})_K \qquad \forall\, v_{N_x,N_y} \in V^{N_x,N_y}.$$

We define the SDFEM-norm by

$$\|v\|_{\rm SD} = \left(\varepsilon|v|_1^2 + \sum_{K\subset\Omega_{11}} \delta_K\|b\cdot\nabla v\|_{0,K}^2 + c_0\|v\|_0^2\right)^{1/2} \quad \forall\, v\in H^1(\Omega).$$

Set $N = \max\{N_x, N_y\}$ and $M = \min\{N_x, N_y\}$. Analogously to [21, p. 305], we set

$$\delta_K = \begin{cases} N^{-1} & \text{if } K\subset\Omega_{11} \text{ and } \varepsilon \leqslant N^{-1},\\ \varepsilon^{-1}N^{-2} & \text{if } K\subset\Omega_{11} \text{ and } \varepsilon > N^{-1}.\end{cases}$$

Using [23, Theorem 4.5] or [27] for $\sigma = 5/2$ in (2.4) we have: There exists a constant C such that the SDFEM solution w_{N_x,N_y} satisfies

$$|\!|\!| I_{N_x,N_y} u - w_{N_x,N_y} |\!|\!|_{\rm SD} \leqslant C(\varepsilon N^{-3/2} + M^{-2}\ln^2 N).$$

Moreover, for the two-scale SDFEM approximation $w^N_{\hat N,\hat N}$ defined by

$$w^N_{\hat N,\hat N} = w_{N,\hat N} + w_{\hat N,N} - w_{\hat N,\hat N}$$

we have for $N_x = N_y = C_2 N^{1/2}$

$$|||u - w^N_{\hat N,\hat N}|||_\varepsilon \leqslant CN^{-1}\ln^2 N.$$

4. Numerical results

In this section we illustrate our theoretical results numerically and also suggest some further possibilities. We consider two examples of (1.1):

Example 1.

$$\begin{aligned} -\varepsilon\Delta u - (2+x)u_x - (3+y^3)u_y + u &= f \quad \text{in } \Omega = (0,1)^2,\\ u &= 0 \quad \text{on } \partial\Omega \end{aligned}$$

with f such that

$$u(x,y) = \cos(x\pi/2)[1-\exp(-2x/\varepsilon)](1-y)^3[1-\exp(-3y/\varepsilon)],$$

and

Example 2.

$$\begin{aligned} -\varepsilon\Delta u - (2+x)u_x - (3+y^3)u_y + u &= f \quad \text{in } \Omega = (0,1)^2,\\ u &= 0 \quad \text{on } \partial\Omega \end{aligned}$$

with f such that $u = S + E_{12} + E_{21} + E_{22}$ with

$$\begin{aligned} S &= (1-x)(1-\mathrm{e}^{-2/\varepsilon})((1-y)^2 + y\mathrm{e}^{-3/\varepsilon}) + (1-y)^2\mathrm{e}^{-2/\varepsilon} + y\mathrm{e}^{-5/\varepsilon},\\ E_{21} &= -((1-y)^2 + y\mathrm{e}^{-3/\varepsilon})\mathrm{e}^{-2x/\varepsilon},\\ E_{12} &= -(1-x+x\mathrm{e}^{-2/\varepsilon})\mathrm{e}^{-3y/\varepsilon},\\ E_{22} &= \mathrm{e}^{(-2x-3y)/\varepsilon}. \end{aligned}$$

In these examples the convective coefficients are negative, unlike (1.3), so the solution has exponential layers at $x = 0$ and $y = 0$. Nevertheless, the theory of our paper is still applicable because the simple change of variables $x \mapsto 1-x$ and $y \mapsto 1-y$ yields a convection-diffusion problem that satisfies (1.3). The right-hand side f is computed via the differential equation using the given function u. In our examples $u \in C^\infty(\Omega)$ and therefore f is sufficiently smooth. The right-hand side f is allowed to be dependent on ε and to have layer terms; it is only important to have a solution decomposition with the properties given in Assumption 2.1.

In our numerical simulations the perturbation parameter is fixed at $\varepsilon = 1\text{E}{-8}$ (except Tab. 3). All calculations are carried out in MATLAB, using biCGstab as solver for the linear systems with an incomplete LU-decomposition. All errors in the tables that follow are measured in the energy norm $\vert\vert\vert \cdot \vert\vert\vert_\varepsilon$ (except Tab. 4).

$\hat N$	N	$\vert\vert\vert u-u^N_{\hat N,\hat N}\vert\vert\vert_\varepsilon$		$\vert\vert\vert u-u_{N,N}\vert\vert\vert_\varepsilon$		$\vert\vert\vert u^N_{\hat N,\hat N}-I_{N,N}u\vert\vert\vert_\varepsilon$		$\vert\vert\vert u^N_{\hat N,\hat N}-I^N_{\hat N,\hat N}u\vert\vert\vert_\varepsilon$		$\vert\vert\vert u-Pu^N_{\hat N,\hat N}\vert\vert\vert_\varepsilon$	
4	16	2.951E−1	0.73	2.690E−1	0.67	1.306E−1	1.39	1.155E−1	1.48	1.434E−1	1.43
8	64	1.070E−1	0.78	1.056E−1	0.77	1.901E−2	1.27	1.485E−2	1.38	1.964E−2	1.29
12	144	5.673E−2	0.81	5.637E−2	0.81	6.810E−3	1.26	4.862E−3	1.40	6.887E−3	1.27
16	256	3.556E−2	0.83	3.542E−2	0.83	3.290E−3	1.27	2.178E−3	1.37	3.308E−3	1.27
20	400	2.457E−2	0.84	2.450E−2	0.84	1.867E−3	1.31	1.181E−3	1.42	1.873E−3	1.31
28	784	1.393E−2	0.86	1.391E−2		7.742E−4	1.32	4.537E−4	1.39	7.755E−4	1.32
40	1600	7.552E−3	0.87			3.019E−4	1.33	1.684E−4	1.36	3.022E−4	1.33
56	3136	4.203E−3	0.88			1.230E−4	1.34	6.751E−5	1.33	1.231E−4	1.34
80	6400	2.242E−3	0.89			4.717E−5	1.34	2.615E−5	1.27	4.718E−5	1.34
112	12544	1.231E−3	0.90			1.916E−5	1.35	1.112E−5	1.28	1.916E−5	1.35
144	20736	7.846E−4				9.729E−6		5.840E−6		9.730E−6	

Table 1. Errors for Example 1, $\hat N = N^{1/2}$, $\varepsilon = 1\text{E}{-8}$.

$\hat N$	N	$\vert\vert\vert u-u^N_{\hat N,\hat N}\vert\vert\vert_\varepsilon$		$\vert\vert\vert u-u_{N,N}\vert\vert\vert_\varepsilon$		$\vert\vert\vert u^N_{\hat N,\hat N}-I_{N,N}u\vert\vert\vert_\varepsilon$		$\vert\vert\vert u^N_{\hat N,\hat N}-I^N_{\hat N,\hat N}u\vert\vert\vert_\varepsilon$		$\vert\vert\vert u-Pu^N_{\hat N,\hat N}\vert\vert\vert_\varepsilon$	
4	16	2.650E−1	0.74	2.384E−1	0.68	1.242E−1	1.44	1.099E−1	1.56	1.366E−1	1.48
8	64	9.471E−2	0.78	9.347E−2	0.77	1.687E−2	1.32	1.272E−2	1.40	1.745E−2	1.34
12	144	5.020E−2	0.81	4.991E−2	0.81	5.801E−3	1.30	4.093E−3	1.35	5.866E−3	1.31
16	256	3.147E−2	0.83	3.136E−2	0.83	2.753E−3	1.31	1.880E−3	1.35	2.767E−3	1.32
20	400	2.175E−2	0.84	2.170E−2	0.84	1.532E−3	1.33	1.027E−3	1.37	1.537E−3	1.34
28	784	1.233E−2	0.86	1.232E−2		6.240E−4	1.35	4.075E−4	1.37	6.249E−4	1.35
40	1600	6.686E−3	0.87			2.383E−4	1.36	1.531E−4	1.37	2.385E−4	1.36
56	3136	3.721E−3	0.88			9.532E−5	1.37	6.081E−5	1.37	9.534E−5	1.37
80	6400	1.985E−3	0.89			3.582E−5	1.38	2.284E−5	1.36	3.583E−5	1.38
112	12544	1.090E−3	0.90			1.419E−5	1.38	9.116E−6	1.36	1.419E−5	1.38
144	20736	6.947E−4				7.089E−6		4.595E−6		7.090E−6	

Table 2. Errors for Example 2, $\hat N = N^{1/2}$, $\varepsilon = 1\text{E}{-8}$.

To begin with, consider the Galerkin FEM. Tabs. 1 and 2 are for Examples 1 and 2 respectively. In them we follow Theorem 3.2 by taking $\hat N = N^{1/2}$; the values of $\hat N$ and N that were used are listed in the first column of each table. Various types of the error E_N are given in columns 2–6, and each column also includes the estimated orders of convergence EOC that correspond to

$$E_N = CN^{-\text{EOC}}.$$

The second column in Tabs. 1 and 2 shows the error of the combination method solution and illustrates clearly the convergence rate forecast by Theorem 3.2. The third column displays the errors for the Galerkin FEM; these errors are close to those of column 2, but of course the combination method uses far fewer points than the Galerkin method while achieving the same degree of accuracy—this is its great strength. Column 3 is shorter than the others because computer memory constraints meant that we could not compute the Galerkin solution $u_{N,N}$ for $N \geqslant 1600$. Column 4 displays the error between the combination method solution and the fine grid interpolant, while the fifth column gives the error between the combination method solution and the two-scale interpolant. A supercloseness property seems to hold true here; we conjecture that the rate of convergence is $\mathcal{O}(N^{-4/3})$.

This apparent supercloseness property leads us to postprocess the combination solution using the technique of [23], where one applies biquadratic interpolation on a macro mesh to the computed solution. The final columns of Tabs. 1 and 2 list the error between the exact solution and the postprocessed solution. The resulting EOCs agree with those of the supercloseness property shown in the fourth column.

Let us investigate whether the errors are uniform in ε. In Tab. 3 we consider Example 1 with $N = 256$ and $\hat{N} = 16$. The perturbation parameter ε takes the values 1, 1E−2, 1E−4, 1E−6, 1E−8, 1E−10. As can be seen, the combination method inherits the ε-uniformity of the Galerkin method on Shishkin meshes. Moreover, it shows that Assumption 2.2 is needed only to simplify the analysis and can be neglected in practice.

ε	$\lvert\lvert\lvert u - u^N_{\hat{N},\hat{N}} \rvert\rvert\rvert_\varepsilon$
1	2.7773E−3
1E−2	3.7145E−2
1E−4	3.5578E−2
1E−6	3.5562E−2
1E−8	3.5562E−2
1E−10	3.5562E−2

Table 3. Errors for Example 1, $N = 256$, $\hat{N} = 16$, ε varying.

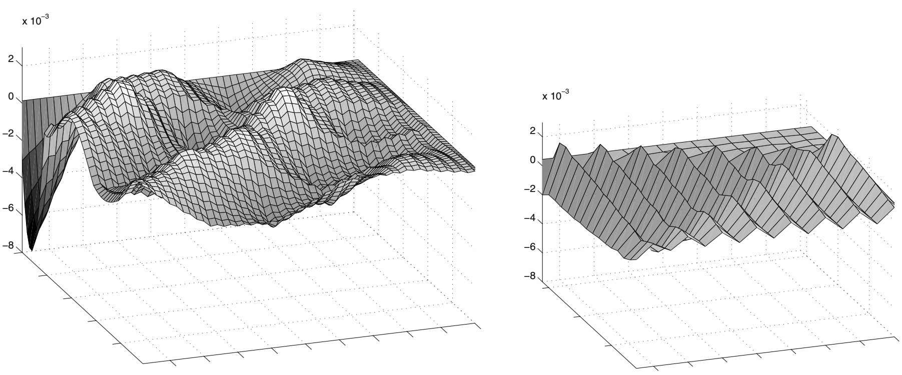

Figure 2. Oscillations inside the coarse mesh region for the combination method (left) and the corresponding Galerkin method (right) for Example 1.

Fig. 2 compares the oscillations in the coarse mesh region Ω_{11}. The combination method solution $u^N_{\hat{N},\hat{N}}$ for $\hat{N} = 10$, $N = 100$ and $\varepsilon = 1\text{E}{-8}$ and the corresponding Galerkin solution $u_{\tilde{N},\tilde{N}}$ for $\tilde{N} = 32$ are computed. In the left picture the difference $u^N_{\hat{N},\hat{N}} - u^I_{N,N}$ is shown in order to highlight the oscillations. In the same way the right picture shows $u_{\tilde{N},\tilde{N}} - u^I_{\tilde{N},\tilde{N}}$. It can be observed that the amplitude of the oscillation is smaller for the combination method.

$\hat{N}$	N	$\Vert u - u^N_{\hat{N},\hat{N}}\Vert_\infty$		$\Vert u - u_{N,N}\Vert_\infty$		$\Vert u^N_{\hat{N},\hat{N}} - I_{N,N}u\Vert_\infty$		$\Vert u^N_{\hat{N},\hat{N}} - I^N_{\hat{N},\hat{N}}u\Vert_\infty$		$\Vert u - Pu^N_{\hat{N},\hat{N}}\Vert_\infty$	
4	16	1.495E−1	0.47	7.764E−2	1.17	1.495E−1	0.47	1.495E−1	0.47	1.203E−2	1.96
8	64	7.793E−2	0.85	1.531E−2	1.44	7.793E−2	0.89	7.793E−2	0.85	7.917E−4	1.35
12	144	3.927E−2	0.69	4.758E−3	1.55	3.794E−2	0.70	3.902E−2	0.73	2.657E−4	1.44
16	256	2.646E−2	0.77	1.952E−3	1.61	2.543E−2	0.72	2.559E−2	0.91	1.161E−4	1.05
20	400	1.879E−2	0.85	9.530E−4	1.65	1.847E−2	0.84	1.705E−2	1.03	7.275E−5	1.20
28	784	1.061E−2	0.96	3.131E−4		1.046E−2	0.95	8.516E−3	1.19	3.249E−5	1.09
40	1600	5.332E−3	1.07			5.302E−3	1.07	3.639E−3	1.34	1.490E−5	1.08
56	3136	2.597E−3	1.17			2.586E−3	1.17	1.473E−3	1.36	7.210E−6	1.09
80	6400	1.126E−3	1.27			1.123E−3	1.27	5.595E−4	1.45	3.315E−6	1.07
112	12544	4.797E−4	1.33			4.791E−4	1.33	2.110E−4	1.59	1.609E−6	1.10
144	20736	2.453E−4				2.450E−4		9.488E−5		9.257E−7	

Table 4. L_∞-errors for Example 2, $\hat{N} = N^{1/2}$, $\varepsilon = 1\text{E}{-8}$.

In Tab. 4 the errors of Table 2 are given in the L_∞ norm. Although we did not prove pointwise convergence results, this table shows that one observes this behavior numerically. Comparing columns three and four, we see that the standard Galerkin method gives better pointwise errors than the combination method.

In Section 3 convergence is only proved for $\hat{N} = C_2 N^{1/2}$. Nevertheless, Theorem 2.6 gives comparable interpolation error estimates for the more economical choice $\hat{N} = C_1 N^{1/3}$. In Tab. 5 we give numerical results for this choice of sparse mesh, showing that similar convergence is attained using fewer points. These results are for Example 1.

$\hat{N}$	N	$\Vert\!\vert u - u^N_{\hat{N},\hat{N}}\vert\!\Vert_\varepsilon$	
4	64	2.604E−1	1.03
6	216	7.431E−2	0.79
8	512	3.762E−2	1.53
10	1000	1.348E−2	0.38
12	1728	1.095E−2	1.36
14	2744	5.835E−3	0.24
16	4096	5.307E−3	0.83
20	8000	3.037E−3	0.85
24	13824	1.906E−3	0.86
28	21952	1.280E−3	0.86
32	32768	9.061E−4	0.88
36	46656	6.650E−4	

Table 5. Errors for Example 1, $\hat{N} = N^{1/3}$, $\varepsilon = 1\text{E}{-8}$.

In the proof of Theorem 3.2 the supercloseness property of the Galerkin method is used. Thus, one could ask: how does this compare with computing the Galerkin solution on a standard Shishkin mesh having the same number of points (i.e., as computationally demanding as the combination method) and applying the postprocessing of [23] to it? In Tab. 6 these two approaches are compared for Example 2. Columns one and four list the number of degrees of freedom used for the combination and Galerkin methods, respectively. Here $\tilde{N}$ is chosen so that $\tilde{N}^2 \approx \hat{N} \times N$. Columns two and five show the errors in the energy norm while columns three and six display the errors of the postprocessed solutions. Clearly the combination method gives better results than the Galerkin method in terms of both the original and postprocessed solutions.

$\hat{N} \times N$	$\vert\vert\vert u - u^N_{\hat{N},\hat{N}} \vert\vert\vert_\varepsilon$	$\vert\vert\vert u - Pu^N_{\hat{N},\hat{N}} \vert\vert\vert_\varepsilon$	$\widetilde{N}^2$	$\vert\vert\vert u - u_{\widetilde{N},\widetilde{N}} \vert\vert\vert_\varepsilon$	$\vert\vert\vert u - Pu_{\widetilde{N},\widetilde{N}} \vert\vert\vert_\varepsilon$
$4 \times 16 = 64$	2.650E−1	1.366E−1	$8 \times 8 = 64$	3.361E−1	1.377E−1
$8 \times 64 = 512$	9.471E−2	1.745E−2	$24 \times 24 = 576$	1.861E−1	3.617E−2
$12 \times 144 = 1728$	5.020E−2	5.866E−3	$40 \times 40 = 1600$	1.317E−1	1.663E−2
$16 \times 256 = 4096$	3.147E−2	2.767E−3	$64 \times 64 = 4096$	9.347E−2	7.903E−3
$20 \times 400 = 8000$	2.175E−2	1.537E−3	$88 \times 88 = 7744$	7.339E−2	4.742E−3
$28 \times 784 = 21952$	1.233E−2	6.249E−4	$148 \times 148 = 21904$	4.883E−2	2.044E−3
$40 \times 1600 = 64000$	6.686E−3	2.385E−4	$252 \times 252 = 63504$	3.177E−2	8.547E−4
$56 \times 3136 = 175616$	3.721E−3	9.534E−5	$420 \times 420 = 176400$	2.083E−2	3.658E−4
$80 \times 6400 = 512000$	1.985E−3	3.583E−5	$716 \times 716 = 512656$	1.330E−2	1.489E−4

Table 6. Combination vs. Galerkin method for Example 2, $\hat{N} = N^{1/2}$, $\widetilde{N} \approx N^{3/4}$, $\varepsilon =$ 1E−8.

$\hat{N}$	N	$\vert\vert\vert u - u^N_{\hat{N},\hat{N}} \vert\vert\vert_\varepsilon$		$\vert\vert\vert u - u_{N,N} \vert\vert\vert_\varepsilon$		$\vert\vert\vert u^N_{\hat{N},\hat{N}} - I_{N,N}u \vert\vert\vert_\varepsilon$		$\vert\vert\vert u^N_{\hat{N},\hat{N}} - I^N_{\hat{N},\hat{N}}u \vert\vert\vert_\varepsilon$		$\vert\vert\vert u - Pu^N_{\hat{N},\hat{N}} \vert\vert\vert_\varepsilon$	
4	16	2.737E−1	0.68	2.688E−1	0.67	7.058E−2	1.07	7.529E−2	1.14	8.105E−2	1.15
8	64	1.065E−1	0.78	1.056E−1	0.77	1.606E−2	1.13	1.548E−2	1.15	1.656E−2	1.16
12	144	5.668E−2	0.81	5.636E−2	0.81	6.437E−3	1.17	6.109E−3	1.18	6.488E−3	1.18
16	256	3.556E−2	0.83	3.542E−2	0.83	3.287E−3	1.19	3.096E−3	1.19	3.298E−3	1.19
20	400	2.458E−2	0.84	2.450E−2	0.84	1.937E−3	1.20	1.818E−3	1.20	1.940E−3	1.20
28	784	1.394E−2	0.86	1.391E−2		8.653E−4	1.20	8.126E−4	1.19	8.659E−4	1.20
40	1600	7.555E−3	0.87			3.671E−4	1.19	3.469E−4	1.18	3.673E−4	1.19
56	3136	4.205E−3	0.88			1.643E−4	1.18	1.567E−4	1.16	1.643E−4	1.18
80	6400	2.242E−3	0.89			7.088E−5	1.16	6.831E−5	1.14	7.089E−5	1.16
112	12544	1.232E−3	0.90			3.256E−5	1.13	3.168E−5	1.12	3.256E−5	1.13
144	20736	7.847E−4				1.841E−5		1.803E−5		1.841E−5	

Table 7. Errors for Example 1 using SDFEM and the combination method, $\hat{N} = N^{1/2}$, $\varepsilon = $ 1E−8.

Finally, let us turn to the SDFEM. Tab. 7 illustrates the results of Remark 3.4. Moreover, as for the Galerkin FEM, the combination method applied to the SDFEM has a supercloseness property. Using a stabilized FEM instead of standard Galerkin reduces the oscillations shown in Fig. 2.

References

[1] *R. E. Bank*: Hierarchical bases and the finite element method. Acta Numerica *5* (1996), 1–43.

[2] *H.-J. Bungartz, M. Griebel*: Sparse grids. Acta. Numerica *13* (2004), 147–269.

[3] *H.-J. Bungartz, M. Griebel, U. Rüde*: Extrapolation, combination, and sparse grid techniques for elliptic boundary value problems. Comput. Methods Appl. Mech. Eng. *116* (1994), 243–252.

[4] *P. G. Ciarlet*: The Finite Element Method for Elliptic Problems. SIAM, Philadelphia, 2002.

[5] *F.-J. Delvos*: d-Variate Boolean interpolation. J. Approximation Theory *34* (1982), 99–114.

[6] *M. Dobrowolski, H.-G. Roos*: A priori estimates for the solution of convection-diffusion problems and interpolation on Shishkin meshes. Z. Anal. Anwend. *16* (1997), 1001–1012.

[7] *J. Garcke, M. Griebel*: On the computation of the eigenproblems of hydrogen and helium in strong magnetic and electric fields with the sparse grid combination technique. J. Comput. Phys. *165* (2000), 694–716.

[8] *M. Griebel, M. Schneider, C. Zenger*: A combination technique for the solution of sparse grid problem. Iterative Methods in Linear Algebra. Proceedings of the IMASS, International symposium, Brussels, Belgium, April 2–4, 1991 (P. de Groen, R. Beauwens, eds.). North-Holland, Amsterdam, 1992, pp. 263–281.

[9] *Q. Lin, N. Yan, A. Zhou*: A sparse finite element method with high accuracy I. Numer. Math. *88* (2001), 731–742.

[10] *T. Linß*: Uniform superconvergence of a Galerkin finite element method on Shishkin-type meshes. Numer. Methods Partial Differ. Equations *16* (2000), 426–440.

[11] *T. Linß*: Layer-adapted meshes for convection-diffusion problems. Comput. Methods Appl. Mech. Eng. *192* (2003), 1061–1105.

[12] *T. Linß, M. Stynes*: Asymptotic analysis and Shishkin-type decomposition for an elliptic convection-diffusion problem. J. Math. Anal. Appl. *261* (2001), 604–632.

[13] *F. Liu, N. Madden, M. Stynes, A. Zhou*: A two-scale sparse grid method for a singularly perturbed reaction-diffusion problem in two dimensions. IMA J. Numer. Anal. To appear.

[14] *F. Liu, A. Zhou*: Two-scale finite element discretizations for partial differential equations. J. Comput. Math. *24* (2006), 373–392.

[15] *F. Liu, A. Zhou*: Localizations and parallelizations for two-scale finite element discretizations. Commun. Pure Appl. Anal. *6* (2007), 757–773.

[16] *F. Liu, A. Zhou*: Two-scale Boolean Galerkin discretizations for Fredholm integral equations of the second kind. SIAM J. Numer. Anal. *45* (2007), 296–312.

[17] *J. J. Miller, E. O'Riordan, G. I. Shishkin*: Fitted Numerical Methods for Singular Perturbation Problems. World Scientific, Singapore, 1996.

[18] *J. Noordmans, P. W. Hemker*: Application of an additive sparse-grid technique to a model singular pertubation problem. Computing *65* (2000), 357–378.

[19] *E. O'Riordan, G. I. Shishkin*: A technique to prove parameter-uniform convergence for a singularly perturbed convection-diffusion equation. J. Comput. Appl. Math. *206* (2007), 136–145.

[20] *C. Pflaum, A. Zhou*: Error analysis of the combination technique. Numer. Math. *84* (1999), 327–350.

[21] *H.-G. Roos, M. Stynes, L. Tobiska*: Numerical Methods for Singularly Perturbed Differential Equations. Springer, Berlin, 1996.

[22] *M. Stynes, E. O'Riordan*: A uniformly convergent Galerkin method on a Shishkin mesh for a convection-diffusion problem. J. Math. Anal. Appl. *214* (1997), 36–54.

[23] *M. Stynes, L. Tobiska*: The SDFEM for a convection-diffusion problem with a boundary layer: Optimal error analysis and enhancement of accuracy. SIAM J. Numer. Anal. *41* (2003), 1620–1642.
[24] *J. Xu*: Two-grid discretization techniques for linear and nonlinear PDEs. SIAM J. Numer. Anal. *33* (1996), 1759–1777.
[25] *H. Yserentant*: On the multi-level splitting of finite element spaces. Numer. Math. *49* (1986), 379–412.
[26] *C. Zenger*: Sparse grids. In: Parallel Algorithms for Partial Differential Equations (Proc. 6th GAMM-Seminar, Kiel, 1990). Notes Numer. Fluid Mech. 31. 1991, pp. 241–251.
[27] *Z. Zhang*: Finite element superconvergence on Shishkin mesh for 2-D convection-diffusion problems. Math. Comput. *72* (2003), 1147–1177.

Authors' addresses: *S. Franz*, Institut für Numerische Mathematik, Technische Universität, Dresden, Germany, e-mail: `sebastian.franz@tu-dresden.de`; *F. Liu*, Central University of Finance and Economics, Beijing, China, e-mail: `fliu@lsec.cc.ac.cn`; *H.-G. Roos*, Institut für Numerische Mathematik, Technische Univeristät, Dresden, Germany, e-mail: `hans-goerg.roos@tu-dresden.de`; *M. Stynes*, National University of Ireland, Cork, Ireland, e-mail: `m.stynes@ucc.ie`; *A. Zhou*, LSEC, ICMSEC, Academy of Mathematics and Systems Science, Chinese Academy of Sciences, Beijing, China, e-mail: `azhou@lsec.cc.ac.cn`.